Reexamination of Tropical Cyclone Wind–Pressure Relationships

JOHN A. KNAFF

CIRA, Colorado State University, Fort Collins, Colorado

RAYMOND M. ZEHR

NOAA/NESDIS, Fort Collins, Colorado

(Manuscript received 16 November 2005, in final form 10 April 2006)

ABSTRACT

Tropical cyclone wind–pressure relationships are reexamined using 15 yr of minimum sea level pressure estimates, numerical analysis fields, and best-track intensities. Minimum sea level pressure is estimated from aircraft reconnaissance or measured from dropwindsondes, and maximum wind speeds are interpolated from best-track maximum 1-min wind speed estimates. The aircraft data were collected primarily in the Atlantic but also include eastern and central North Pacific cases. Global numerical analyses were used to estimate tropical cyclone size and environmental pressure associated with each observation. Using this dataset (3801 points), the influences of latitude, tropical cyclone size, environmental pressure, and intensification trend on the tropical cyclone wind–pressure relationships were examined. Findings suggest that latitude, size, and environmental pressure, which all can be quantified in an operational and postanalysis setting, are related to predictable changes in the wind–pressure relationships. These factors can be combined into equations that estimate winds given pressure and estimate pressure given winds with greater accuracy than current methodologies. In independent testing during the 2005 hurricane season (524 cases), these new wind–pressure relationships resulted in mean absolute errors of 5.3 hPa and 6.2 kt compared with the 7.7 hPa and 9.0 kt that resulted from using the standard Atlantic Dvorak wind–pressure relationship. These new wind–pressure relationships are then used to evaluate several operational wind–pressure relationships. These intercomparisons have led to several recommendations for operational tropical cyclone centers and those interested in reanalyzing past tropical cyclone events.

1. Introduction

Possibly the most accurate and reliable measure of tropical cyclone (TC) intensity is the minimum sea level pressure (MSLP) either estimated from aircraft reconnaissance flight level or obtained via direct observation (surface or dropwindsonde). However, the destructive potential of TCs is better related to the maximum wind speed at or near the surface. For this reason, TC forecasts and advisories as well as climatological records are most useful when they describe TC intensity in terms of maximum surface wind speed (10-m level, 1-min sustained, 10-min average, etc.)—a difficult quantity to measure. This reality has led to the development of relationships between the MSLP and maximum surface wind speed, which are used both operationally and in postanalysis of individual TC events. While these "wind–pressure relationships" attempt to describe the mean relationship between the MSLP and maximum wind, the actual relationship is a function of several factors related to TC environment and structure that vary from case to case. As a result, there is considerable scatter about any given wind–pressure relationship (WPR).

Since TCs are well approximated by the gradient wind balance (Willoughby 1990; Willoughby and Rahn 2004), one need only examine the cylindrical form of the gradient wind equation in azimuthal mean and integral form to better understand what factors determine the MSLP in a TC (Hess 1959):

$$\mathrm{MSLP} = P_{\mathrm{env}} - \int_{r=0}^{r_{\mathrm{env}}} \rho\left(\frac{V_t^2}{r} + fV_t\right) dr. \qquad (1)$$

Corresponding author address: John Knaff, CIRA, Colorado State University, Fort Collins, CO 80523-1375.
E-mail: knaff@cira.colostate.edu

DOI: 10.1175/WAF965.1

Two obvious factors are size, which is given by the radius of the environmental pressure, (r_{env}) and environmental pressure (P_{env}). A more subtle factor is the integral of $\rho[(V_t^2/r) + fV_t]$, where V_t is the tangential wind, ρ is density, and f is the Coriolis force [$f = 2\Omega \sin(\phi)$, where ϕ is latitude]. This integral term accounts for a number of factors (radius of maximum winds, secondary wind maxima, etc.) that are difficult to accurately measure operationally and climatologically, particularly in the absence of aircraft reconnaissance data. The authors concede that in some circumstances the radius of maximum winds can be accurately estimated using satellite techniques and quite often when aircraft reconnaissance is available. Nonetheless, any variation in the radial profile of the tangential wind will change the MSLP and in turn may greatly influence how MSLP is related to the maximum surface wind.

In a modern operational setting with satellite imagery and quality global analyses, five basic factors that affect the WPR can always be estimated in operations: size, latitude, environmental pressure, storm motion, and intensification trend. The first two, size and latitude, determine the potential magnitude of the integral in Eq. (1). Storm motion has been shown to slightly influence the maximum surface wind speeds associated with TCs resulting in slightly greater intensities for faster-moving storms if all other factors are held constant (Schwerdt et al. 1979). The intensification trend has also been shown to be an important factor for the slope of the WPR (Koba et al. 1990). This is likely due to the shape of the radial profiles of the tangential wind being a function of intensification trend.

In the situation when aircraft reconnaissance is available, there is less of a need for WPRs, as the flight-level winds, a proxy for surface winds, and MSLP are measured independently. Surface winds are routinely estimated from flight level [e.g., as described in Franklin et al. (2003)], though there is still uncertainty in such estimates. Thus, WPRs can provide additional independent information when other techniques (i.e., satellite-based intensity estimates) have estimated either the MSLP or maximum surface wind speeds. This application, however, may be more important during the post-operational reanalysis of storm intensity.

Historically, WPRs have been derived primarily by making use of two methods. The first is to assume cyclostrophic balance:

$$V_t^2 = \frac{r}{\rho}\frac{\partial p}{\partial r}, \tag{2}$$

where r is the radius, p is pressure, and ρ density. In application, a loose approximation of cyclostrophic balance,

$$V_{max} = C(P_{ref} - P_c)^n, \tag{3}$$

is most often applied, where P_{ref} is a reference pressure, P_c is the MSLP, C is an empirical constant, and n is an empirical exponent—noting that $n = 0.5$ represents cyclostrophic balance. In this methodology, historical data are used to find the best fit to parameters C and n. However, as Landsea et al. (2004) point out, since the numbers of weaker cases often outnumber the stronger cases, one should bin the cases by intensity before finding the best fit. The second common methodology makes uses of maximum wind speed or MSLP composites. However, the development of WPRs in the past has been most challenged by the relatively few cases available for their development rather than by what methodology is used to fit the data.

Five different WPRs have been used at the operational TC centers throughout the world. They are the following:

1) Atkinson and Holliday (1977, 1975), used at the Regional Specialized Meteorological Center (RSMC) on La Reunion island, RSMC Fiji, the Perth tropical cyclone center, and at the Joint Typhoon Warning Center;
2) Koba et al. (1990) used at the RSMC Tokyo;
3) Love and Murphy (1985) used in the Australian Northern Territory tropical cyclone warning center in Darwin;
4) a method attributed to Crane used at the Brisbane tropical cyclone warning center (Harper 2002); and
5) Dvorak (1975) (i.e., the Atlantic part of the table column in Fig. 5) is used for the Atlantic and east Pacific at the National Hurricane Center/Tropical Prediction Center (NHC/TPC) and for the central Pacific at the Central Pacific Hurricane Center.

These relationships are shown in Fig. 1a in terms of $\Delta P = (\text{MSLP} - P_{env})$. Also shown in Fig. 1b are the four WPRs used by Landsea et al. (2004) for the Atlantic best-track reanalysis (1850–1910) in terms of $\Delta P = (\text{MSLP} - 1013)$. All of the operational WPRs, except that of Atkinson and Holliday (1977, hereafter AH), were compiled using composite methods, most used relatively limited datasets, and all were developed more than 15 yr ago. For a more comprehensive review of the history of WPRs and the individual wind versus pressure methodologies, reading Harper (2002) is recommended. However, two historical points from Harper (2002) are important to the remainder of this paper. First, unlike the development of other WPRs and despite the laborious task of assembling the AH dataset, AH did not bin their data by intensity before creating a best fit. Second, the Dvorak (1975) WPRs

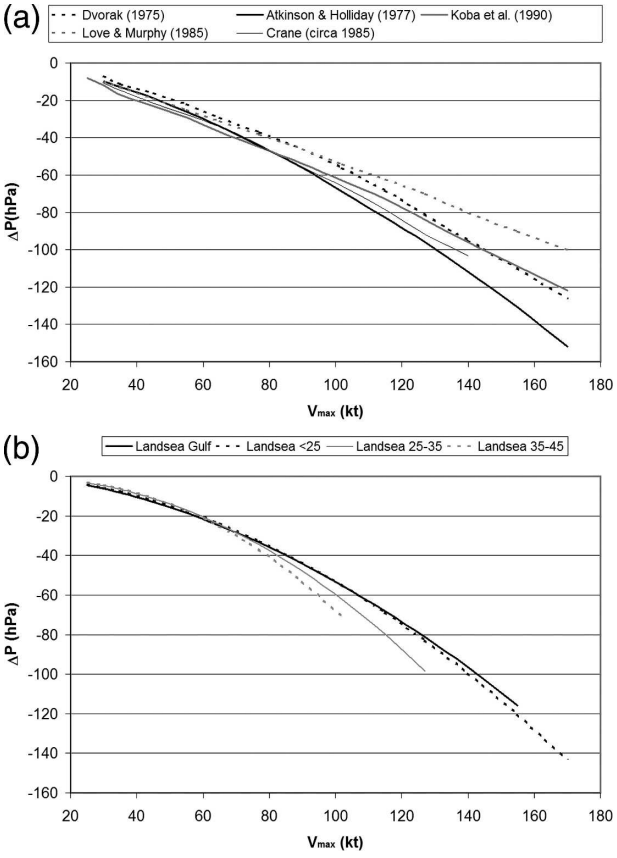

FIG. 1. Comparison of (a) the WPRs used at operational centers throughout the world and (b) the WPRs used by Landsea et al. (2004) as discussed in the text. Note all winds speeds are given in terms of 1-min sustained winds and that the Dvorak CI number is used to compare WPRs where 10-min average winds are the standard (e.g., Fiji, Japan, and Australia).

are derived primarily from western Pacific MSLP measurements and are identical save for the offset of 6 hPa to account for the lower environmental pressure in the western North Pacific.

Given the curves in Fig. 1, it is only natural to question the relative accuracy of these methods and ask whether or not one can develop better techniques with a greater number of cases and with more recently collected datasets. One consideration is that more recent best-track data that take into account near-surface wind measurements from GPS dropwindsondes (circa 1997) as well as flight-level to surface wind reduction factors developed using GPS dropwindsonde information (Franklin et al. 2003), which have been used in operations since ~2002. However, it is worth noting that the flight-level to surface wind reduction factors have varied somewhat during the period of analysis. Also available are quality reanalyses of atmospheric conditions (Kalnay et al. 1996), which can be used to estimate TC size and environmental conditions. It is also now know that TCs are closely approximated by the gradient wind balance (Willoughby 1990) and that the cyclostrophic balance is a less accurate balance approximation.

In addition to the operational considerations, the estimates of WPRs have become the basis of some of the TC intensity climatology. For instance, in the past it was routine to estimate the MSLP from aircraft and then assign the winds according to that pressure. Any errors or biases in these past estimates remain in the current best-track intensity estimates. Such errors and biases as well as others resulting from changes in operational procedures have become particularly important with recent publications showing dramatic upward trends in the intensities of global TCs (i.e., Emanuel 2005; Webster et al. 2005).

With the above factors in mind, the aim of this paper is to better understand the scatter between MSLP and TC maximum wind speeds, use this knowledge to evaluate operational WPRs, and to make recommendations based on those assessments. To this end, composites of the WPR stratified by size, latitude, and intensity trend are created. It is important to note that since the systematic differences between TC basins (latitude, size, and P_{env}) are explicitly accounted for in this methodology, the resulting WPRs are applicable to any TC. The pressure observations come from aircraft data and the maximum wind speeds are interpolated to the time of the pressure observation from the best track. A unified regression approach will be developed from the composites. Finally, using this unified approach, the WPRs used in operations and for best-track and climatological reanalyses will be examined, and recommendations made.

2. Datasets

This is a 15-yr study (1989–2004) that makes use of three separate datasets: aircraft MSLP estimates or dropwindsonde measurements in the eye, TC best tracks, and National Centers for Environmental Prediction–National Center for Atmospheric Research (NCEP–NCAR) reanalysis and analysis fields. Aircraft intensity fixes are maintained in a digital database that is part of the Automated Tropical Cyclone Forecast (ATCF) system (Sampson and Schrader 2000). Each aircraft intensity fix has a time (nearest minute), location (nearest 10th of a degree), and intensity MSLP (nearest hPa) associated with it. These fixes are the foundation for this study and are the points in time and space by which environmental pressure and cyclone size are estimated. Aircraft fixes are mostly located in the Atlantic TC basin, but there are a few (N = 268)

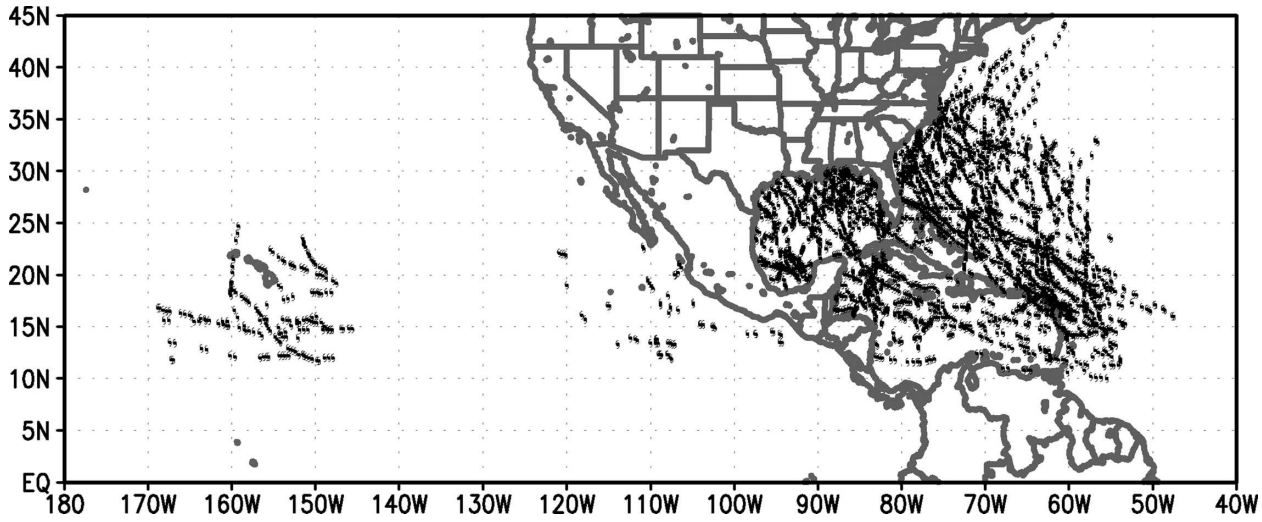

FIG. 2. Geographical location of the tropical cyclone fixes used in this study. Each hurricane symbol represents a fix.

storm fixes available in the central and eastern North Pacific. Fixes within 30 km of land are not used in this study to limit the effects of landfall-induced intensity change. Figure 2 shows the location of the points (N = 3801) used in this study. Tropical cyclone maximum wind speeds in the operational advisories and historical TC databases are given to the nearest 5 kt (1 kt = 0.52 m s^{-1}). For this reason, the nonstandard unit of knots is used for wind speeds throughout this paper. For the remainder of this paper $V_{\max}$ refers to the 1-min sustained 10-m wind speed in units of knots, as is the convention at the NHC. To better compare western North Pacific WPRs, similar fixes containing the MSLP data collected by aircraft reconnaissance are utilized (1966–87).

Tropical cyclone best tracks are created following the TC season and include the best estimate of location and intensity every 6 h (Jarvinen et al. 1984). The best tracks are archived in an ATCF database and are available from the National Hurricane Center. Maximum wind speeds and storm translation speeds are interpolated to the aircraft fix time from 6-hourly values in the best-track files. Maximum wind 12 h prior to the aircraft fix time is also calculated in the same manner. The 12-h intensity trend is then easily calculated. Figure 3 is a plot of the wind speeds reported in the best tracks versus the maximum 10-s wind reported at flight level within 3 h of the best-track time in the U.S. Air Force aircraft reconnaissance data 1995–2004, which were observed using a common flight pattern at standardized heights. The high correlation (R^2 = 0.90) between these datasets indicates that best-track estimates of maximum winds are influenced by flight-level wind values in a systematic manner. Best-track data from the western North Pacific, maintained by the Joint Typhoon Warning Center (JTWC), are used in the evaluation operational WPRs in that region (JTWC 2006).

The translation speed (c) of a storm has a small influence on the maximum surface winds in a TC, and it is desirable to remove this influence for this study. To remove this influence of the storm motion, a storm-relative maximum surface wind speed (V_{srm}) is estimated by $V_{\text{srm}} \approx V_{\max} - 1.5c^{0.63}$ as suggested by Schwerdt et al. (1979). This approximation assumes that the maximum winds are to the right of the TC motion in the Northern Hemisphere, which is the case

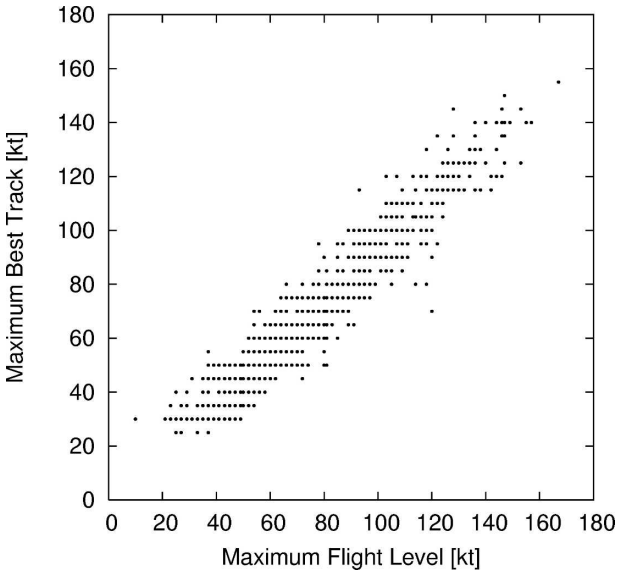

FIG. 3. Comparison between the maximum sustained 1-min winds in the best track vs the maximum 10-s wind reported at flight level for 1995–2004.

with flight-level winds (Mueller et al. 2006) that are often used in operations to estimate V_{max}. The maximum surface wind's location is still a point of scientific debate (e.g., Kepert 2001; Kepert and Wang 2001).

Six-hourly NCEP analyses are used to estimate the TC size and environmental sea level pressure conditions for each aircraft fix. Operational analyses are used for years 2001 to present and NCEP–NCAR reanalysis fields are used prior to that time.

Since it is the gradient of the pressure that is best related to the wind field, the environmental pressure in which a TC is embedded should be accounted for in any study of TC WPRs. An environmental pressure for each fix is estimated by calculating the azimuthal mean pressure in an 800–1000-km annulus surrounding the cyclone center at each adjacent reanalysis time. To make the calculation, the MSLP is interpolated to a finer grid (10 km). These interpolated values are then averaged if they fall within the 800–1000-km annulus. The final estimate is determined by interpolating the 6-hourly estimates to the time of the aircraft fix. Using this estimate of environmental pressure (P_{env}), a pressure deficit (ΔP) is estimated by subtracting P_{env} from the MSLP provided by the aircraft fix.

In an operational setting, TC size is described by the radial extent of gale force winds or the radius of the outermost closed isobar. Both quantities are estimated by the warning agency, which for most cases in this study is NHC. The size can also be evaluated by the wind fields in the reanalysis data. Ideally, the size would be quantified according to the radius of the zero tangential winds; however, this quantity is very difficult to determine. Fortunately, the average tangential winds calculated from the NCEP analyses in the annulus of 400–600 km (V_{500}), calculated in the same manner as P_{env}, correlate with TC size. The tangential winds in this annulus are not only resolved by the global numerical analyses, but often correspond with the radial extent of the cirrus canopy (Kossin 2002; Knaff et al. 2003). Figure 4 shows the relationship ($R^2 = 0.25$) between V_{500} and the average radius of 34-kt winds reported in the NHC advisories (1995–2004). Additionally, it is recognized that TC size is also influenced by differences in intensity and latitude [see Eq. (1)]. To evaluate a range of tropic cyclone sizes for differing intensities and locations, a normalized size parameter is developed.

To remove the influence of TC intensity and latitude from the size estimate, the V_{500} is then divided by the value by the climatological tangential wind 500 km from the center (V_{500c}), which is estimated using a modified rankine vortex:

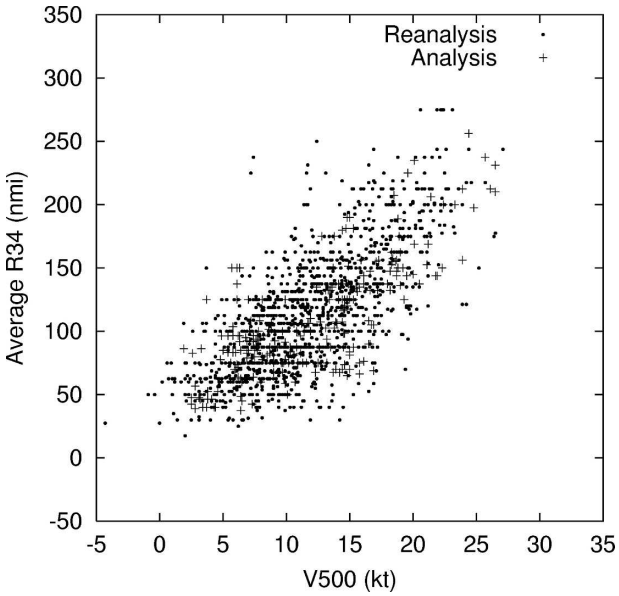

FIG. 4. The mean storm-relative tangential velocity calculated from the NCEP analyses and the NCEP–NCAR reanalysis fields vs the average radius of 34-kt winds reported in the NHC advisories. The average is the mean radius of the nonzero quadrants for each advisory. Note that TC size and P_{env} are estimated from the NCEP–NCAR reanalysis fields during 1989–2000, and from the NCEP operational analysis fields during 2001–04.

$$V_{500c} = V_{max}\left(\frac{R_{max}}{500}\right)^{x}, \tag{4}$$

where x, the shape factor, and R_{max}, the radius of maximum winds in kilometers, are functions of latitude (ϕ) in degrees and intensity (V_{max}) in knots:

$$x = 0.1147 + 0.0055V_{max} - 0.001(\phi - 25) \quad \text{and} \tag{5}$$

$$R_{max} = 66.785 - 0.09102V_{max} + 1.0619(\phi - 25). \tag{6}$$

Coefficients for this modified Rankine vortex model are derived from the operational Atlantic wind radii Climatology and Persistence (CLIPER) model discussed in Gross et al. (2004). These equations are valid for $V_{max} \geq 15$ kt.

For each aircraft fix, a value of V_{500} is estimated by interpolating values calculated at adjacent analysis times to the time associated with the fix. The value of V_{500} is then normalized by dividing this value by V_{500c}.

In summary, aircraft fixes for the period (1989–2004) collected in the Atlantic and central and eastern North Pacific provide a date and time, location, and MSLP associated with various TCs. Aircraft fixes within 30 km of land are excluded from the dataset. Using the times and locations of the remaining fixes, the best-track maximum winds, 12-h trends and intensities, and 12-h

TABLE 1. Mean statistics of the individual composites.

Sample	No.	Avg lat (°)	Avg size	Avg V_{max}	Avg V_{max} trend	Avg P_{env}	Avg speed (kt)	Avg MSLP
Whole	3801	23.67	0.49	72.15	2.55	1014.25	9.61	979.61
<20°	1226	16.51	0.48	74.86	1.99	1013.18	10.00	979.45
20°–30°	1917	24.94	0.48	71.30	3.42	1014.27	9.07	979.74
>30°	659	33.33	0.52	69.57	1.04	1015.18	10.44	979.52
Small	595	23.43	0.18	59.16	2.44	1015.12	9.81	992.74
Avg	2562	23.43	0.47	69.70	3.03	1014.18	9.68	982.03
Large	644	24.88	0.83	93.90	0.71	1013.72	9.14	957.84
Weakening/steady	1746	24.27	0.51	73.16	−5.66	1014.48	9.60	977.97
Intensifying	2056	23.17	0.47	71.30	9.52	1014.06	9.62	980.99

motion are interpolated to the time of each fix. The effects of storm motion are removed then from the intensity estimate to form a storm-relative maximum surface wind, V_{srm}. Similarly, NCEP analyses are used to estimate the environmental sea level pressure at 800–1000 km (P_{env}) and the average tangential winds at 400–600 km (V_{500}) associated with each fix. The influence of the P_{env} is then subtracted from each MSLP fix to form a pressure deficit (ΔP). The estimate of V_{500} is divided by a climatological value [Eqs. (4)–(6)] to form a normalized TC size parameter, which is used to estimate and account for variations in TC size. Combining this information results in 3801 cases with estimates of time, location, MSLP, P_{env}, ΔP, V_{max}, V_{srm}, 12-h trends of V_{max}, 12-h motion, and TC size. These parameters are used in the following sections to reexamine TC WPRs.

3. Methodology

There are five basic factors that affect the WPR considered in this study that can be both estimated with current datasets and in an operational setting. These include environmental pressure, storm motion, latitude, storm size, and intensification trend. In the following section, each of these factors will be discussed. Other factors, associated with the radial distribution of tangential winds, particularly variations in the radius of maximum wind (RMW), are not considered.

Statistics associated with each composite and the whole dataset are shown in Table 1. Individual composites are created by binning V_{srm} every 2.5 kt for V_{srm} values less than or equal to 70 kt and every 5 kt for V_{srm} values above 70 kt. In the cases where there are less than 10 individual cases in a bin, those cases are combined with the next ascending bin(s) until at least 10 cases are utilized in each average. Detailed results of these stratifications will be discussed in section 4.

Using the composites based upon latitude, size, and intensity trend, which are binned by intensity, regression equations are developed for each composite using predictors that closely approximate the likely best fit associated with gradient wind balance (i.e., $\Delta P \approx aV_{srm}^2 + bV_{srm} + C$). The deviation from historical practice is justified by our current knowledge that TCs are well approximated by gradient balance rather than cyclostrophic balance. These equations then will be used to estimate the value of ΔP for each Dvorak current intensity (CI) number given in appendix B.

In addition, the composite averages of each of the individual composites are used to create one unifying regression equation that can be used to predict ΔP as a function of V_{max}, latitude, size, and intensity trend. Likewise, regression equations will be developed for V_{max} (i.e., $V_{srm}(\Delta P) = a\Delta P + b\sqrt{|\Delta P|} + C$, and $V_{max} = V_{srm} + 1.5c^{0.63}$, where c is storm motion), but only for those stratifications that would be used for climatological reanalysis. These unified approaches will be discussed in section 5. These unified regression equations will be compared with techniques used both operationally throughout the world and for best-track reanalysis activities in section 6.

4. Factors influencing wind–pressure relationships

a. Environmental pressure

For the 3801-case dataset, the mean value of P_{env} is 1014.3 hPa, the standard deviation is 2.5 hPa, the maximum is 1025.1 hPa, and the minimum is 1004.5 hPa. Figure 5, which shows MSLP versus V_{max} and ΔP versus V_{max}, illustrates the effect of using ΔP instead of MSLP when developing WPRs. There is a very small reduction (i.e., 0.3%) in the variance explained by a linear fit of ΔP compared to MSLP, and the resulting scatter in Fig. 5b is still substantial.

b. Storm motion

Storms that translate at faster speeds have been shown to have slightly larger maximum surface

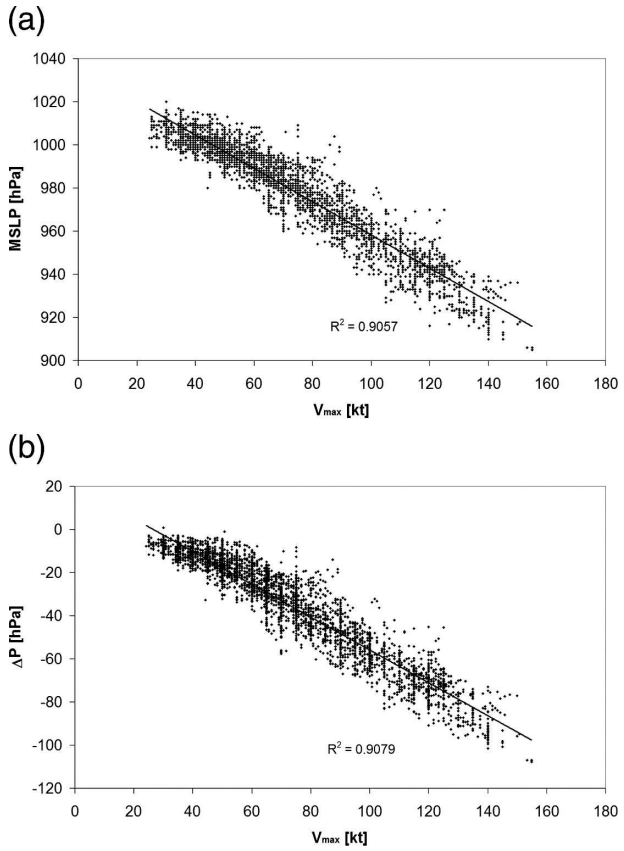

FIG. 5. Scatterplots of (a) MSLP vs V_{max} and (b) ΔP vs V_{max}.

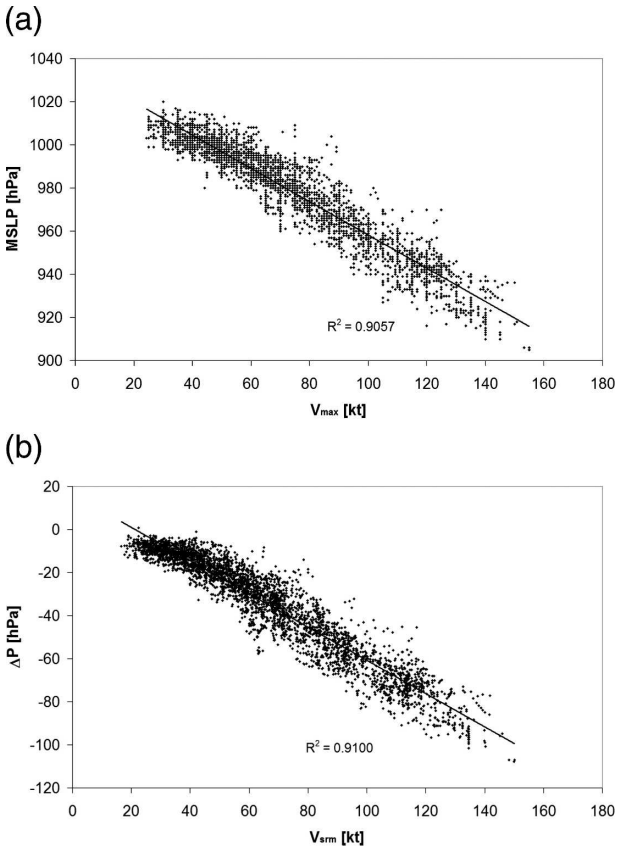

FIG. 6. Scatterplots of (a) ΔP vs V_{max} and (b) ΔP vs V_{srm}.

(Schwerdt et al. 1979) and flight-level winds (Mueller et al. 2006). Storm motion in this sample had a mean value of 9.6 kt with a standard deviation of 4.6 kt and ranged from 0 to 34.8 kt. Figure 6 shows the scatter diagram of ΔP versus V_{max} and ΔP versus V_{srm}, the effect of removing this factor on the WPR. Again, as was the case with removing the effects of P_{env}, removing the influence of storm motion has a relatively small effect on the reduction of the scatter, increasing the variance explained by about 0.2%.

c. Latitude

As latitude increase, the Coriolis force also increases, requiring lesser tangential wind to balance the pressure gradient force. As a result, higher-latitude storms have lower pressures given the same radial wind profile. To explore the influence of latitude in our dataset, composites are constructed. The average latitude of the whole sample is 23.7°N with a standard deviation of 6.4°. Latitude-based composites are constructed from fixes for regions equatorward of 20° latitude, between 20° and 30° latitude, and greater than 30° latitude. This resulted in 1226, 1970, and 659 cases, respectively. The mean quantities of the individual composites are shown in Table 1.

The composite results of the latitudinal stratification (Fig. 7) show that the ΔP versus V_{srm} relationship is clearly a function of latitude. The differences seem fairly systematic for V_{srm} values greater than 45 kt. In this intensity range, there is approximately a 5-hPa decrease for every 10° of latitude. These composites confirm that for a given V_{srm} a low-latitude storm will on average have higher values of ΔP.

d. Size

Following the gradient wind balance, large TCs have smaller V_{max} for a given ΔP because the pressure gradient is distributed over a larger radial distance. Figure 8 shows the relationship between the size parameter (i.e., V_{500}/V_{500c}) and the average radius of 34-kt winds from the advisories. The size parameter explains 40% of the variance of the average radius of 34-k winds (the sample mean radius of 34-kt winds is 110 n mi). As a test to see if the size parameter was really indicating size, we examined the tails of the distribution for storms with $V_{max} > 100$ kt. The largest storms with these in-

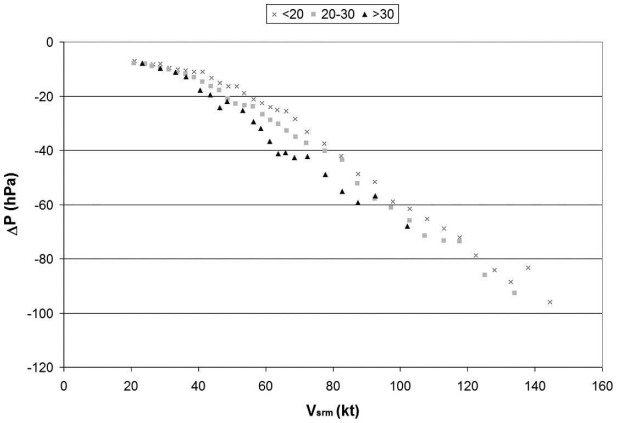

FIG. 7. Plots of ΔP vs V_{srm} for the three latitudinal composites.

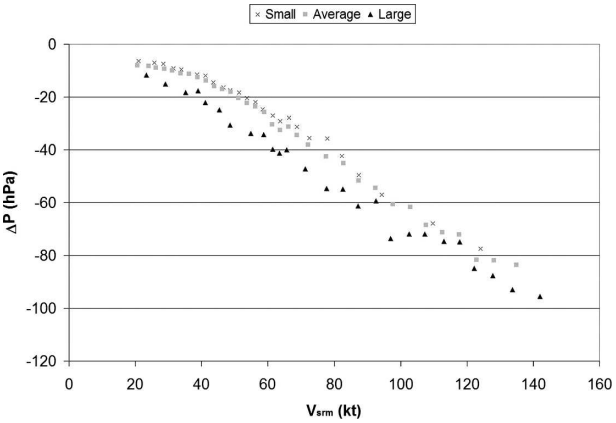

FIG. 9. Plots of ΔP vs V_{srm} for the three size-based composites.

tensities were all from the Atlantic: Isabel (2003), Floyd (1999), Luis (1995), Gert (1995), and Mitch (1999)—all notably large storms. The smallest storms were Charlie (2004) and Andrew (1992) from the Atlantic, John (1994, south of Hawaii) and Olivia (1994) from the east Pacific, and Iniki (1992) from the central Pacific—all notably small storms. Examining the seasonal summaries and other information available about these storms, it appears that the size parameter is providing a good estimate of TC size. Further evidence is presented in the composite means.

Based on this size parameter, three composites are created containing small, average, and large storms. The distribution of this TC size measure is nearly normal with a mean value of 0.49 and a standard deviation of 0.22. The composites consist of those cases less than 1 standard deviation from the mean (small), between +1 and −1 standard deviations from the mean (average), and those cases with sizes greater than 1 standard deviation from the mean (large) resulting in 595, 2562, and 644 cases, respectively. Further size stratification (e.g., that used in Merrill 1984) was not attempted as the number of large TC cases became too small. Again, mean quantities associated with each composite are shown in Table 1.

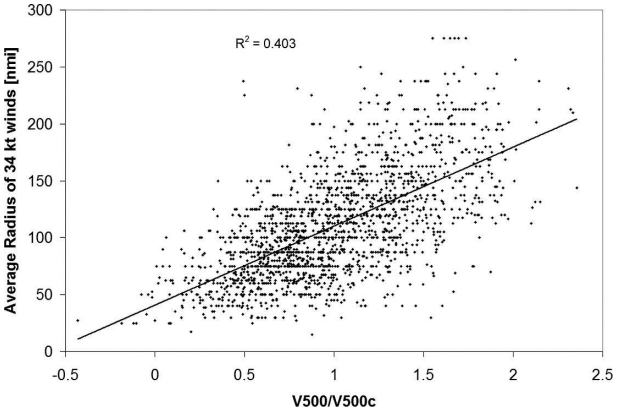

FIG. 8. A plot of the relationship between the TC size parameter (V_{500}/V_{500c}) and the average 34-kt wind radii from operational advisories (1989–2004).

The WPRs resulting from the composite averages are shown in Fig. 9. Interestingly, the differences between small TC and average-sized TC composites are rather small, but for the large storms, 16.9% of the sample, ΔP tended to be significantly lower than storms with similar V_{srm}. In Fig. 9, there appears to be a slight discontinuity in the large composite cases occurring in the intensity range 85–120 kt that requires further explanation. This was examined and is related to the mean latitude of the composite averages stratified by intensity. As the intensity increased, the mean latitude decreased from ~28° at 85 kt to ~20° at 125 kt.

e. Intensity trend

Koba et al. (1990), using surface MSLP and satellite wind estimates gathered in the western North Pacific, found that the WPR was also a function of intensity trend. The steady and weakening (intensifying) storms tended to have lower (higher) pressures at intensities below 65-kt strength (i.e., Dvorak T-number ~5.5) and higher (lower) pressures above this threshold. These trends may be the result of the TC life cycle and typical structural differences (vortex size and radius of maximum winds) between developing and decaying TCs (i.e., those discussed in Weatherford and Gray 1988). Composites of steady and weakening storms are compared with those that are weakening, repeating the analysis of Koba et al. (1990). Mean statistics associated with these composites are shown in Table 1.

Composite averages based on intensity trends are shown in Fig. 10. These data confirm the results re-

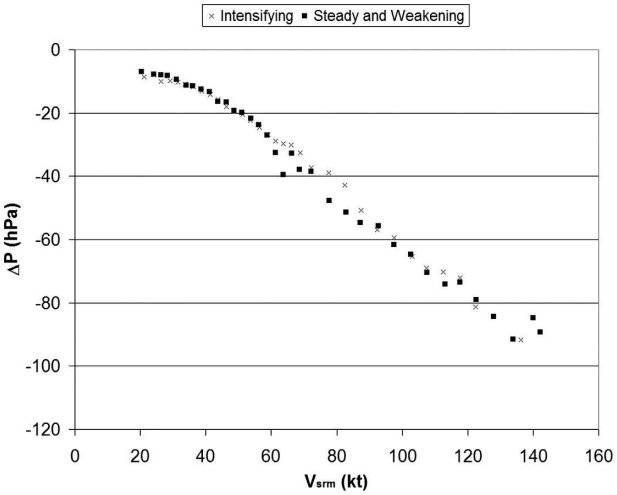

FIG. 10. Plots of ΔP vs V_{srm} for the two intensity trend-based composites.

ported in Koba et al. (1990) that showed that weakening/steady and intensifying storms have different WPRs. The shapes of these curves suggest that the intensity trend of a given storm is an important factor in determining the WPR.

Using independent data, the differences found by Koba et al. (1990) were confirmed here. Findings show that weakening/steady (intensifying) storms have a tendency to have lower (higher) pressures below intensities of ~40–65 kt and higher (lower) pressures at intensities greater than ~40–65 kt. However, examining the composite results with respect to trend also shows that the intensifying storms are smaller and at lower latitude than the weakening storms in the same ranges of maximum wind speed in which the WPR has the greatest differences. Figure 11 shows the average size and average latitude versus the storm-relative maximum wind for the intensifying and weakening/steady composites. Furthermore, these relationships have been fit to second-order polynomials shown by the black and gray lines, which shows that there are clearly size and latitude differences between these composites. These results suggest that the differences in the WPRs between intensifying and weakening systems are likely due to differences in size and latitude between intensifying and weakening storms. Several studies have shown that the circulations associated with TCs become larger the longer the storm exists (Cocks and Gray 2002; Weatherford and Gray 1988; Merrill 1984). The results suggest that the majority of storms intensify early in their life cycle when on average they are smaller and at lower latitude and weaken latter in their life cycle when they are larger and at higher latitude. The results however suggest that it is the size differences that are most

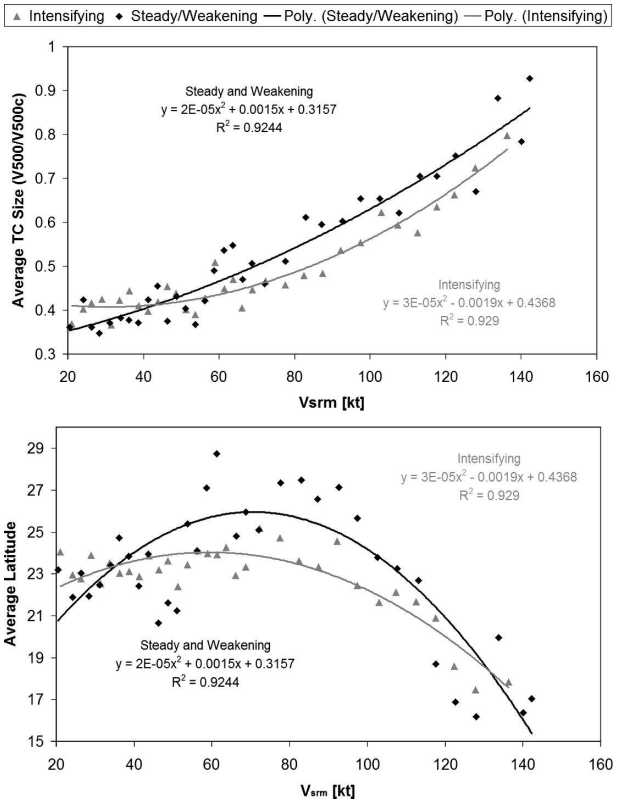

FIG. 11. Composites of average storm-relative maximum surface winds (V_{srm}) vs (top) composite average TC size and (bottom) average tropical cyclone latitude. Composites are stratified by 12-h intensity trends. The averages of storms with steady or weakening (intensifying) intensity trends are shown by the black (gray) points. Second-order polynomial trend lines are added with the same shading.

important. In the intensity range of 64–100 kt the sizes are ~0.30 standard deviations smaller for the intensifying composite, but only a couple of degrees latitude equatorward. This result will be examined further in the next section discussing the development of unified WPRs.

5. Unified wind–pressure relationships

A unified WPR to predict MSLP is derived using multiple linear regressions where the predictors tested are TC size, latitude, and intensification trend. The intensity trend predictor, while added as a potential predictor in the multiple regression approach, resulted in less than a 0.01% reduction of the variance when latitude and size were included as predictors. For this reason, intensity trend is not considered. This further emphasizes that intensity trend is not independent of the

factors size and latitude. The resulting multiple regression equation is

$$\mathrm{MSLP} = 23.286 - 0.483V_{\mathrm{srm}} - \left(\frac{V_{\mathrm{srm}}}{24.254}\right)^2 - 12.587S - 0.483\phi + P_{\mathrm{env}}, \quad (7)$$

where V_{srm} is the maximum wind speed adjusted for storm speed, S (i.e., $= V_{500}/V_{500c}$) is the normalized size parameter discussed in section 3, and ϕ is latitude (in °). When applied to the individual cases used to make the composites, this equation explains 94% of the variance with a root-mean-square error (RMSE) of 5.8 hPa and a mean absolute error (MAE) of 4.4 hPa. For comparison, the standard Dvorak curve for the Atlantic explained 91% of the variance with an RMSE of 7.1 hPa and an MAE of 5.4 hPa.

One could solve Eq. (7) for V_{srm}, but analogous to solving for the gradient wind, the solution has two roots. The WPR can also be derived as a separate regression equation to estimate V_{max} given ΔP. In the development of this regression equation, the square root of ΔP is used as a predictor in addition to ΔP, size, and latitude:

$$V_{\mathrm{max}} = 18.633 - 14.960S - 0.755\phi - 0.518\Delta P + 9.738\sqrt{|\Delta P|} + 1.5c^{0.63}, \quad (8)$$

where c is the storm translation speed. Applying this relationship to the individual fixes explains 93% of the variance of the wind speed and results in an MAE of 6.0 kt and an RMSE of 7.8 kt. Again for comparison, the Atlantic Dvorak curve explains 90% of the variance, with an MAE of 7.6 kt and an RMSE 9.8 kt. Because S is a function of V_{max}, a good estimate of V_{max} is needed; otherwise, Eq. (8) should be iterated to a solution of V_{max}. Convergence within 1 kt is usually obtained in two iterations.

The WPRs developed in this section [i.e., Eqs. (7) and (8)] account for the influence of TC size and latitude, storm motion, and environmental pressure when estimating MSLP and V_{max}. Figure 12 shows the dependent relationships from Eqs. (7) and (8). Both relationships can be used in operations to help with the assignment of V_{max}, given a measurement of MSLP, and to estimate MSLP when V_{max} has been estimated (e.g., Dvorak intensity estimates). Since there is still considerable uncertainty with the various observations (satellite estimates, reconnaissance wind reduction, wind averaging periods, etc.), these equations can also be used to add consistency to operational V_{max} and MSLP estimates. Furthermore, since both Eqs. (7) and (8) account for P_{env}, TC size, and latitude—the same factors that account for the differences between TC basins, then these equations can be applied to any TC basin. Under that premise, these relationships are used in the next section to examine other WPRs used at operational centers.

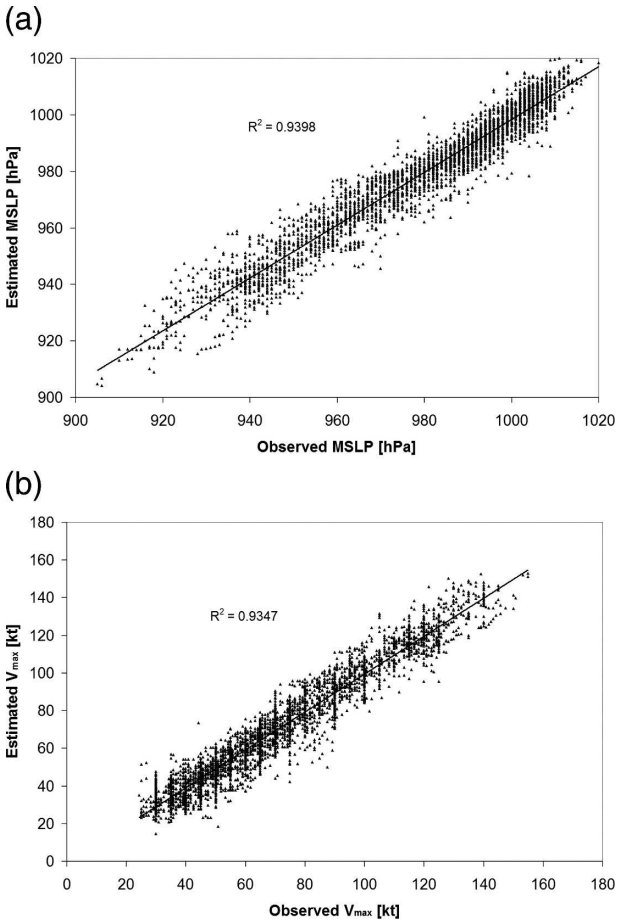

FIG. 12. The dependent results of (a) Eq. (7) for predicting MSLP given V_{max} and (b) Eq. (8) for estimating V_{max} given MSLP.

A possibly more important use of these equations is to offer an improved way to estimate intensities for the climatological reanalysis of TC intensities. There is an increasing need to reanalyze the best-track intensities in all basins since these historical records are being used to assess climate change (e.g., Webster et al. 2005; Emanuel 2005). While the Atlantic basin best track including intensity has been reanalyzed from 1850 to 1910 (Landsea et al. 2004), future reanalysis of these intensities will be aided by the results presented here. With this type of application in mind, section 7 presents a comparison of results generated by Eq. (8) with the method used in Landsea et al. (2004).

TABLE 2. Statistics associated with Eq. (7) using the observed environmental pressure (P_{env}), Eq. (16) using the climatological environmental pressure (P_{clim}) from the sample, and the Atlantic Dvorak, Koba et al. (1990), AH, Love and Murphy (1985), and Crane WPRs. Bias and error statistics that are statistically different than those produced by Eq. (7) are shown in italics for the 95% and boldface for the 99% levels, respectively.

	Eq. (7) P_{env}	Eq. (7) P_{clim}	Dvorak Atlantic	Koba et al. (1990)	AH	Love and Murphy (1985)	Crane
Bias	−0.5	−0.5	*0.9*	**−7.0**	**−8.2**	−1.2	**−7.9**
RMSE	5.8	6.3	*7.1*	**9.9**	**11.5**	**8.1**	**10.6**
MAE	4.4	4.8	*5.4*	**8.2**	**9.1**	**6.4**	**8.8**

6. Reexamination of operational wind–pressure relationships

The first operational WPR examined is from Dvorak (1975, 1984) for the Atlantic, which is used for estimating MSLP in the Atlantic and eastern and central Pacific. To examine the Dvorak (1975) Atlantic WPR, the published tables were fit to a function MSLP = $1021.36 - 0.36V_{max} - (V_{max}/20.16)^2$, which introduces an MAE of 0.7 hPa, an RMSE of 0.8 hPa, and a bias of 0.1 hPa to the Dvorak WPR table. The developmental data were then passed through this function. The results are then compared with MSLP computed from Eq. (7) using the observed environmental pressure as well as the sample average environmental pressure for P_{env}. Those results were then compared with the observed MSLP and MAE, RMSE, and bias, shown in Table 2. Results that are statistically different, assuming 211 degrees of freedom (df) [i.e., df = $-n \log(r_1)$, where r_1 is the lag 1 autocorrelation] and a standard two-tailed student's t test, from those produced by Eq. (7) are set in italics (95% level) and boldface (99% level) in the table.

Using Eq. (7) along with the observed environmental pressure led to improvement over the Atlantic Dvorak WPR relationship. Even the use of mean environmental pressure in Eq. (7) instead of the observed environmental pressure yielded slightly better results. The effectiveness of the Dvorak WPR is however remarkable considering that it was developed using mostly western Pacific data, but adjusted upward for the average differences in environmental pressure (Harper 2002). There is however a couple of caveats associated with these results. The first is that the Dvorak WPR is used operationally in these basins and there may be a built-in dependence (i.e., using this relationship to assign V_{max} some of the time) as suggested by Harper (2002). The second is that Eq. (7) is not completely independent. Independent results are presented later in this paper.

The next operational WPR examined is that of Koba et al. (1990). Using a similar approach, the tabular values of ΔP (assuming P_{env} = 1010 hPa) were fit to a function, $\Delta P = 6.22 - 0.58V_{max} - (V_{max}/31.62)^2$, where V_{max} is the 1-min sustained wind associated with the Dvorak CI number. Thus, this study does not consider the conversion of 1- to 10-min averaging times used in Koba et al. (1990) or by the Japanese Meteorological Agency. This function introduces an MAE of 0.8 hPa, an RMSE of 0.9 hPa, and a bias of 0.4 hPa to the Koba et al. WPR table. These are then compared to Eq. (7) in a similar manner as before. The results and statistical significance of this comparison are shown in Table 2. The Koba et al. (1990) relationship is not a good relationship for these data because it has a large and systematic bias. A closer inspection of the biases shows that they are very similar to the changes in ΔP seen between composites of average and small TCs compared with large TCs. This result along with the observation that TCs in the western Pacific are generally larger than those in the Atlantic (Merrill 1984) suggest that the Koba et al. (1990) sample is generally of larger storms. If only the storms in the large composite are considered, the Koba et al. (1990) WPR seems good (i.e., not statistically significant at the 90% level); the RMSE is 7.0 hPa and the MAE is 5.7 hPa with a bias of −2.2. For comparison, Eq. (7) produced an RMSE of 8.1 and an MAE of 6.6 and had a bias of −5.3 for the large-storm sample. Indirectly, this further implies that the Koba et al. dataset likely consisted of generally larger storms.

The next WPR examined is the AH, which should have similar properties to the Koba et al. (1990) WPR (i.e., similar to the large composite sample). Again, 1010 hPa is used for the environmental pressure and the published function is $\Delta P = -(V_{max}/6.7)^{1.553}$. The error statistics associated with the application of this WPR to this study's data and its rather poor performance are shown in Table 2. Since the Koba et al. (1990) results suggest that the western Pacific sample may contain larger storms, error statistics are also calculated for the large composite data; the RMSE is 12.5 hPa and the MAE is 9.67 hPa with a bias of −7.4 hPa—all of which are statistically significant at the 99% level. These values are very similar to the comparison with the whole dataset, suggesting that the AH WPR may not be as valid as either Eq. (7) or the Koba et al. (1990) WPR.

Interestingly, there is a negative bias throughout the entire intensity range with the largest errors occurring for very intense storms. The estimates of ΔP made by the AH WPR tend to be 20 hPa too low for V_{max} above 120 kt. It therefore appears that the AH WPR is a bad fit. This last point is expanded upon in appendix A where the raw AH data are reexamined.

In Australia there are different WPRs used at each TC forecast office. Perth uses the AH WPR; Darwin uses the Love and Murphy (1985) WPR, where $\Delta P = 6.37 - 0.54V_{max} - (V_{max}/43.03)^2$; and Brisbane uses a WPR table attributed to Crane $\Delta P = 5.82 - 0.50V_{max} - (V_{max}/22.20)^2$. The errors introduced by creating functional forms are an MAE of 0.4 hPa, an RMSE of 0.52 hPa, and a bias of 0.4 hPa for the Love and Murphy WPR and an MAE 0.7 hPa, an RMSE of 1.0 hPa, and a bias 0.7 hPa for the Crane WPR. Using the same methodologies as above, both of these WPRs are compared with results from Eq. (7) as shown in Table 2.

The Love and Murphy WPR produces good error statistics, but the overall biases are a result of large negative biases associated with weaker storms and large positive biases, particularly above intensities of 90 kt (i.e., Dvorak T-number = 5.0). Since cyclones forecast by Darwin tend to be at low latitudes and small, this WPR is similar to that of Guard and Lander (1996), which was created specifically for midget TCs. To examine the regional latitude effect, this WPR is then compared with the low-latitude composite cases. Doing so resulted in similar statistics that are statistically significant at the 95% level: an RMSE of 8.9 hPa and an MAE 7.4 hPa, with a bias of −4.0 hPa, compared to an RMSE of 7.4, an MAE of 5.9, and a bias of −4.5 from Eq. (7). Similarly, a comparison was made with the small composite data resulting in an RMSE of 8.7 hPa, an MAE of 7.2 hPa, and a bias of −5.4 hPa compared to an RMSE of 7.0 hPa, an MAE of 5.1 hPa, and a bias of −3.3 hPa. These differences too were significant at the 95% level.

The WPR used at Brisbane has characteristics similar to those of the AH WPR (Harper 2002) and as shown in Fig. 1. Error statistics for this WPR are shown in Table 2. Inferring a similarity with the western Pacific, this scheme was also examined using the large composite resulting in a bias of −5.1 hPa, an RMSE of 9.45 hPa, and an MAE of 7.5 hPa. Thus, this methodology has performance characteristics similar to those of the AH WPR.

In summary, there are five WPRs used in operations throughout the world. Each was examined for their ability to perform better than the relationship given in Eq. (7). One of the five methods, the Atlantic Dvorak performed well when compared to results produced by Eq. (7). The Dvorak Atlantic relationship from Dvorak (1975, 1984) produced good results for the entire developmental dataset. Two other relationships performed well for subsets of the developmental data. The Koba et al. (1990) relationship is valid for a large-sized subset of storms and the Love and Murphy (1985) WPR relationship seems valid for the combination of small and low-latitude storms, though Eq. (7) provides a better fit to the developmental data. The WPR attributed to Crane used at the Brisbane tropical cyclone center performed poorly versus the developmental sample and other size-based subsamples, and thus a change in operational WPRs should be considered.

Finally, the AH WPR has a large negative bias in V_{max} for intense storms that does not seem to be supported by our dataset nor by the developmental dataset used in Koba et al. (1990). This result suggest that the replacement of the Dvorak (1975) western Pacific WPR table by that of AH in Dvorak (1984) may have been unjustified. Given the rather limited justification for the use of AH in the western Pacific (i.e., Shewchuk and Weir 1980; Lubeck and Shewchuk 1980), and the results from the Koba et al. (1990) WPR presented here, the use of the AH WPR appears to be unsupported by the data. The problem with this method can be attributed to the methodology used to fit the data, as discussed in appendix A. In regions where the AH WPR is used, its use should be reconsidered with the possibility of replacing it with Eq. (7), the Koba et al. (1990) WPR, or at very least the western Pacific WPR table published in Dvorak (1975).

Furthermore, regarding recent climatological studies, evidence suggests that the use of the AH WPR to assign wind speeds given the aircraft estimate of MSLP has resulted in a systematic wind speed bias (too low) in the western Pacific TC climatology during the time of its use at JTWC (~1974–87). Figure 13 shows the MSLP estimated from aircraft versus the best-track wind speeds in the western North Pacific for 1966–73 and 1974–87 along with the best fit to the data and the AH WPR. In operations, it was routine that surface winds were assigned using the observed MSLP in WPRs. This figure shows that in the later period (1974–87) the AH WPR is used to assign maximum surface wind speeds. This results in the western North Pacific best-track intensity estimates being too low in the years 1974–87, particularly for the more intense storms. These findings offer an alternative explanation for some of the upward trends in TC intensity reported in the northwest Pacific (Emanuel 2005; Webster et al. 2005). Ironically, this implies that the western Pacific best-track V_{max} estimates for the stronger storms may have become more

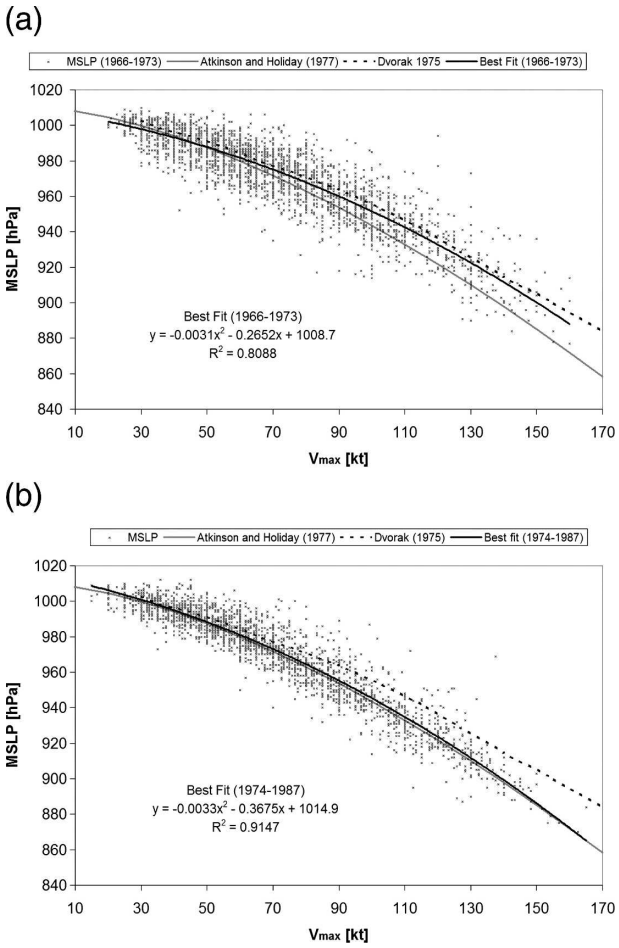

FIG. 13. MSLP vs best-track maximum surface winds (V_{max}) interpolated to the time of the observations and the associated best fit relationships to these data for (a) 1966–73 and (b) 1974–87. Also shown are the AH and Dvorak (1975) WPRs.

accurate without aircraft reconnaissance, somewhat contradictory to the results of Martin and Gray (1993).

7. Wind–pressure relationships used for climatological reanalysis

While operational users usually assign a pressure given a wind, the opposite is done when meteorologists reanalyze TC intensities. Often there is an observed or estimated MSLP from reconnaissance or surface/ship observations, but no or limited measures of the TC wind speed. The tabular forms of the operational tables are sometimes used to do this type of reanalysis, but as shown above, these operational tables sometimes result in considerable bias and error. Equation (8) offers an alternative to the operational tables and can be iterated to a stable solution for V_{max} given MSLP.

Recently, the Atlantic best tracks were reanalyzed and extended backward in history for the period 1851–1910. There were four WPRs used for this reanalysis (Landsea et al. 2004), which were developed from the aircraft era of the best-track dataset (1970–97) in regions known to have routine reconnaissance. These WPRs (shown in Fig. 1b) will now be examined in a similar way as the WPRs used in the operations, but with respect to V_{max} [i.e., Eq. (8)] for comparisons. These comparisons again make use of the observed environmental pressure and the sample mean or climatological pressure.

Results of this analysis are shown in Table 3. In the region south of 25°N, both the Landsea et al. relationship and Eq. (8) performed well with slightly negative biases and MAEs below 7.5 kt. It is interesting to note that the use of the observed environmental pressure south of 25°N resulted in significant improvements to both schemes. In the Gulf of Mexico, Eq. (8) outperforms the Landsea et al. equations, and again the use of environmental pressure results in smaller errors in Eq. (8) as well as the Landsea et al. equation. Results from Eq. (8) are shown to produce superior results in the Atlantic regions between 25° and 35°N. In this region, the use of the observed environmental pressure has a negative effect on the Landsea et al. relationships. In the region poleward of 35°N, Eq. (8) is again superior to the Landsea et al. approach. Also notice that there is more scatter in the data (i.e., larger RMSE) suggesting more size and environmental pressure variability in this poleward of 35°N group. As a result, errors associated with both Eq. (8) and the Landsea et al. relationships increase dramatically in this higher-latitude region. For comparison, the Atlantic Dvorak tables produced an RMSE of 9.8 kt, an MAE of 7.6 kt, and a bias of 0.8 kt for the entire developmental dataset.

In summary, the Landsea et al. equations do an admirable job of estimating the winds from the pressure equatorward of 25°N, while the Landsea et al. WPRs for Atlantic storms north of 25°N and for the Gulf of Mexico have larger errors and lower correlation than those produced by Eq. (8). In all cases, the results from Eq. (8) improve on the Landsea et al. equations. This suggests that environmental pressure and cyclone size play a factor in the WPR, particularly north of 25°N, and should be considered when reanalyzing TC intensity since 1948 when TC size estimates are available from the NCEP–NCAR reanalysis data.

8. Independent results from 2005

To better ascertain the accuracy of Eqs. (7) and (8), an independent dataset from the entire 2005 hurricane season is used to evaluate these equations. Similar results were also calculated using the Atlantic tables in Dvorak (1975, 1984). Results, shown in Table 4, suggest

TABLE 3. Statistics (R^2, bias, RMSE, and MAE) associated with Eq. (8) using the observed environmental pressure (P_{env}), Eq. (8) using the climatological environmental pressure (P_{clim}) from each regional subsample along with the appropriate Landsea et al. (2004) regional WPRs utilizing a reference pressure either equal to 1013 or P_{env}. Bias and error statistics that are statistically different than those produced by Eq. (8) are shown in italics for the 95% and boldface for the 99% levels, respectively.

	South of 25°N, N = 1540, df = 85			
	Eq. (8) using P_{env}	Eq. (8) using P_{clim} = 1013.6	Landsea et al., P_{ref} = 1013	Landsea et al., P_{ref} = P_{env}
R^2	0.95	0.93	0.92	0.94
Bias	−.1.04	−1.29	**−2.32**	−1.13
RMSE	7.67	*8.68*	**9.54**	8.04
MAE	5.89	*6.55*	**7.29**	6.20
	Gulf of Mexico, N = 818, df = 45			
	Eq. (8) using P_{env}	Eq. (8) using P_{clim} = 1013.5	Landsea et al., P_{ref} = 1013	Landsea et al., P_{ref} = P_{env}
R^2	0.93	0.92	0.89	0.91
Bias	−0.94	−1.13	**1.78**	**2.88**
RMSE	7.34	8.05	*9.16*	8.34
MAE	5.53	6.10	**7.22**	*6.72*
	25°–35°N, N = 1011, df =56			
	Eq. (8) using P_{env}	Eq. (8) using P_{clim} = 1015.8	Landsea et al., P_{ref} = 1013	Landsea et al., P_{ref} = P_{env}
R^2	0.93	0.93	0.90	0.91
Bias	−1.25	−1.50	**1.95**	**6.25**
RMSE	7.64	*8.87*	**9.81**	**10.03**
MAE	6.01	6.75	**7.65**	**8.34**
	North of 35°N, N = 165, df = 9			
	Eq. (8) using P_{env}	Eq. (8) using P_{clim} = 1016.3	Landsea et al., P_{ref} = 1013	Landsea et al., P_{ref} = P_{env}
R^2	0.83	0.79	0.60	0.46
Bias	0.14	0.09	**4.85**	**8.21**
RMSE	7.71	8.93	10.18	*11.73*
MAE	6.27	7.15	*8.74*	*9.68*

that the equations developed here perform significantly better than the operational Dvorak WPR. Pressures (winds) are more accurate by approximately 2 hPa (3 kt) for this 524-case sample.

Figure 14 shows predicted V_{max} given the MSLP using Eq. (8) and the Dvorak WPR versus the final best-track V_{max} estimate (top) and the predicted MSLP using Eq. (7) and the Dvorak WPR versus aircraft measurement of MSLP (bottom). The scatters associated with the estimates made with Eqs. (7) and (8) are smaller and the estimates have a better one to one correspondence with the observations than those making use of the Dvorak WPR. It is also noteworthy that the largest outliers (30 kt and 27 hPa) were associated with Hurricane Wilma, which at that time had a 2 n mi radius of maximum winds and 892-hPa MSLP. Large overestimation of V_{max} and underestimation of MSLP occurred with Hurricane Rita as its radius of maximum winds appeared to shrink as it approached land; in fact its MSLP was a record low for a storm hitting the coast with 100-kt winds. The errors associated with these two independent cases suggest that information about the radius of maximum winds could likely improve these relationships even further.

9. Summary and recommendations

The purpose of this work was to reexamine the issue of TC WPRs using more recently collected and higher quality datasets along with additional environmental factors that are measurable in an operational setting. While it is recognized that other factors (i.e., radius of maximum wind, secondary wind maxima, flight level to surface wind reduction, asymmetries, and other radial wind profile variations) will influence the MSLP relationship to the wind, these factors are not easily and

TABLE 4. Independent comparison of results obtained from Eqs. (7) and (8) vs the operational Dvorak tables. Data include 491 fixes from 12 Atlantic tropical cyclones and 1 eastern Pacific tropical cyclone during the 2005 season. Bias and error statistics that are statistically different are shown in italics for the 95%, and boldface for the 99% levels, respectively.

	Independent comparison, N = 524, df = 29			
	Eq. (7) for ΔP	Dvorak ΔP	Eq. (8) for V_{max}	Dvorak V_{max}
R^2	0.95	0.91	0.95	0.92
Bias	**1.55**	**4.43**	**1.14**	**4.69**
RMSE	**7.50**	**10.58**	**6.13**	**11.55**
MAE	**5.30**	**7.67**	**5.06**	**9.02**

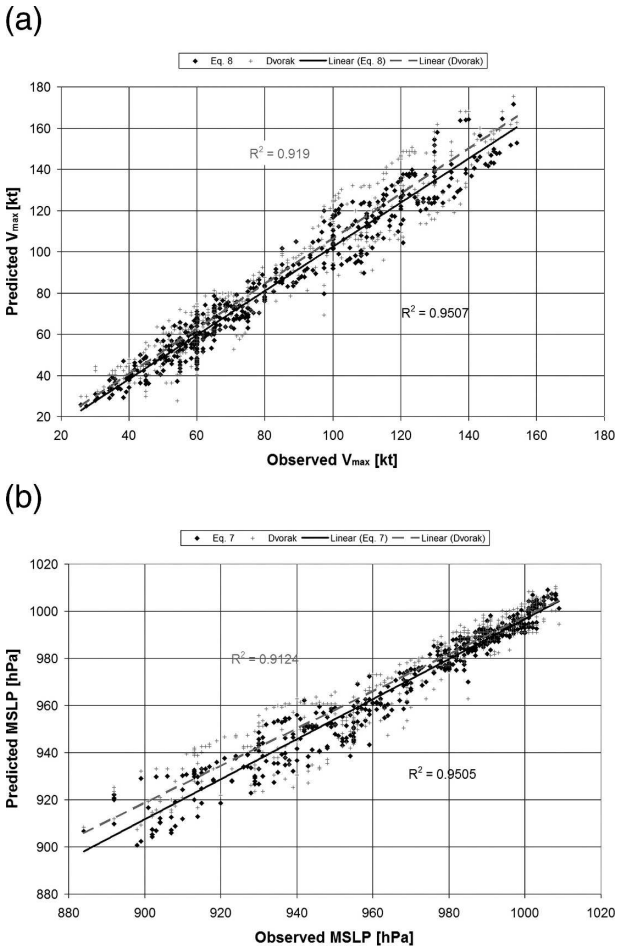

FIG. 14. (top) Scatter diagram of the independently predicted values of V_{max} using Eq. (8) (black boxes) and the Dvorak WPR (crosses) vs observed values of MSLP from the operational best track. (bottom) A similar scatter diagram for Eq. (7) (black boxes) and the Dvorak WPR (crosses) vs observed MSLP. Best linear fits for Eqs. (8) and (7) are shown with a solid black line in each respective panel with the associated variance explained at the bottom right. Best linear fits for the Dvorak WPR are shown by the gray dashed lines with the associated variance explained in the upper left. Sample includes 524 cases.

accurately obtained in either an operational setting and/or only occasionally in a postanalysis setting. Such factors therefore were not considered in this study. As a result, there is still considerable scatter in these new WPRs when these factors, particularly variations of the radius of maximum wind, are influencing the WPR.

Results indicate that by using information about TC location (i.e., latitude) along with estimates of size and of environmental pressure estimated from operational analysis or reanalysis fields, the MSLP can be estimated from the V_{max} within 5–6 hPa and the wind can be estimated from the MSLP within 7–8 kt. These relationships have been shown to be better than what is being used operationally and for the reanalysis of past events. In addition, the data have shown that several operational WPRs have substantial shortcomings and their operational use should be reconsidered. It was also found that the equations used to reanalyze Atlantic TCs (i.e., Landsea et al. 2004) preformed rather well equatorward of 25°N. Estimates of winds in the open Atlantic poleward of 25°N and in the Gulf of Mexico result in significantly larger errors than the methodology presented here [i.e., Eq. (8)].

Wind–pressure relationships have left their mark on the global TC climatology in those basins that had routine aircraft reconnaissance and thus good estimates of MSLP. Fortunately, the actual WPRs used and the methodologies used to assign V_{max} have evolved and improved, but this has resulted in considerable errors and inconsistencies in the best-track intensities of the past. This is an important point because the best-track intensities are now being examined for climatic trends (e.g., Webster et al. 2005; Emanuel 2005). While the WPRs presented in this paper still result in considerable scatter, their application to past data will nonetheless result in an objective and homogeneous measure of TC intensity. Only by removing the inhomogeneous nature of best-track intensities, whether by this method or some other method, can climatic trends in numbers and intensities be properly quantified.

The results of this study also inspire the following recommendations. 1) The unified equations for the WPR should be considered for operational use in all basins. This would help better assign the MSLP, which is provided to initialize forecast models, as well as result in uniform intensity estimates. 2) The AH WPR and the Crane WPR, which are similar, should be replaced in all basins currently using these relationships. Further justification is given in appendix A. 3) The western Pacific best tracks should be reanalyzed during the period when reliable measurements of MSLP were available. Doing so would likely increase the number of strong typhoons (1974–87) and thus reduce the upward intensity trends observed in the best track (1970–2004) as discussed in Webster et al. (2005) and Emanuel (2005). 4) The unifying equations [Eqs. (7) and (8)] should be utilized to reanalyze the best tracks in the Atlantic when the NCEP–NCAR reanalysis and MSLP estimates are available (1948–present). This would help to provide a more consistent and accurate estimate of maximum surface winds in the best-track dataset.

Acknowledgments. This research was supported by NOAA Grant NA17RJ1228. The views, opinions, and findings contained in this report are those of the authors and should not be construed as an official Na-

TABLE A1. Biases and MAE associated with the various fits to the raw Atkinson and Holliday (1975) dataset. Listed here are the (1) published AH WPR, (2) the cyclostrophic form fit to the binned AH data, (3) the gradient fit for the binned AH data, and for comparison (4) the gradient fit to the Koba et al. (1990) WPR.

	(1) AH	(2) Cyclostrophic fit to binned data	(3) Gradient fit to binned data	(4) Koba et al. (1990)
MAE	6.64	5.88	5.80	5.80
Bias	−0.69	1.64	0.36	0.77

tional Oceanic and Atmospheric Administration or U.S. government position, policy, or decision. The authors thank the three anonymous reviewers for their suggestions and comments, which have improved the paper. The authors also would like to thank Bruce Harper for providing the digital Atkinson and Holliday (1975) dataset used in appendix A.

APPENDIX A

The Atkinson and Holliday Wind–Pressure Relationship Revisited

The AH WPR is reexamined using the original tabular data listed in Atkinson and Holliday (1975). The first step is reproducing the prior result. Using the raw data, the function $V_{max} = C(1010 - MSLP)^x$ was fit to see if the original relationship could be reproduced. The results of this fit, $V_{max} = 6.6(1010 - MSLP)^{.65}$, were slightly different than the publish version (i.e., $V_{max} = 6.7(1010 - MSLP)^{.644}$, but close enough to confirm that the AH WPR was fit to the raw data without first binning by intensity.

To examine the effect of binning the data, the raw data are sorted by V_{max}, binned every six points and refit to the same function. The result, $V_{max} = 4.4(1010 - MSLP)^{.76}$, is much different from the original published fit. Finally, the functional form used previously in this paper is fit (i.e., $\Delta P \approx aV_{srm}^2 + bV_{srm} + C$) so that direct comparison with the WPR of Koba et al. (1990) can be made. The results, $\Delta P = 11.48 - 0.73V_{max} - (V_{max}/107.21)^2$, are nearly identical to, while slightly more linear than, the fit to the WPR table published in Koba et al. (1990) (i.e., $\Delta P = 6.22 - 0.58V_{max} - (V_{max}/31.62)^2$. It also is found that the all of formulations that make use of the binned data and the Koba et al. WPR produce a better fit to the raw data than does the AH WPR equation. Table A1 shows the relevant error statistics associated with each fit.

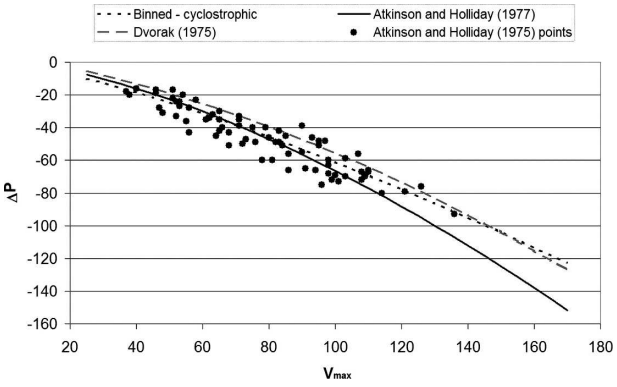

Figure A1. Various WPRs plotted along with the Atkinson and Holliday (1977, 1975) developmental data. WPRs shown are the AH, a fit to the binned raw data assuming a cyclostrophic form, and the Dvorak (1975). To plot these curves in terms of ΔP, 1010 hPa is assumed to be the environmental reference pressure.

TABLE B1. Dvorak CI vs ΔP tables for storms occurring equatorward of 20° latitude.

	Small	Avg	Large
CI	ΔP	ΔP	ΔP
1.5	−2	−4	−8
2.0	−4	−7	−11
2.5	−7	−10	−14
3.0	−13	−16	−20
3.5	−20	−22	−27
4.0	−27	−29	−34
4.5	−35	−38	−42
5.0	−45	−48	−52
5.5	−55	−58	−62
6.0	−66	−69	−73
6.5	−76	−79	−84
7.0	−88	−92	−96
7.5	−103	−106	−111
8.0	−118	−122	−126

TABLE B2. Dvorak CI vs ΔP tables for storms occurring betweem 20° and 30° latitude.

	Small	Avg	Large
CI	ΔP	ΔP	ΔP
1.5	−4	−8	−12
2.0	−7	−11	−15
2.5	−10	−14	−18
3.0	−16	−20	−24
3.5	−23	−26	−31
4.0	−30	−33	−38
4.5	−38	−42	−47
5.0	−48	−52	−56
5.5	−58	−62	−66
6.0	−69	−73	−77
6.5	−80	−83	−88
7.0	−92	−96	−100
7.5	−107	−110	−115
8.0	−122	−126	−130

TABLE B3. Dvorak CI vs ΔP tables for storms occurring poleward of 30° latitude.

	Small	Avg	Large
CI	ΔP	ΔP	ΔP
1.5	−8	−12	−16
2.0	−11	−15	−19
2.5	−14	−18	−22
3.0	−20	−24	−28
3.5	−27	−30	−35
4.0	−33	−37	−42
4.5	−42	−46	−50
5.0	−52	−56	−60
5.5	−62	−66	−70
6.0	−73	−77	−81
6.5	−84	−87	−92

The bias introduced by the AH WPR is clearly shown in Fig. A1, which shows the published AH WPR, the fit to the binned Atkinson and Holliday (1975) data assuming cyclostrophic form, and the Dvorak (1975) WPR for intensities from 25 to 170 kt. Note that the other WPRs developed using the binned data discussed above as well as the Koba et al. WPR are nearly identical (within 1 hPa) to the cyclostrophic fit shown in Fig. A1. This last point is remarkable because the V_{max} data in AH were likely overestimated, particularly at elevated sites (Harper 2002). Figure A1 alone suggests that the prolonged use of the AH WPR in the western Pacific (1974–87) has resulted in a negative bias in the best-track intensities.

APPENDIX B

Dvorak CI Curves for Various Composites

From a combination of Eqs. (7) and (8) and the composite averages, Dvorak WPR tables are formulated in terms of current intensity (CI) number versus ΔP. Three tables are listed for the three latitude belts used in this study. Tables B1, B2, and B3 are valid for storms located equatorward of 20°, from 20° to 30° latitude, and for greater than 30° latitude, respectively.

REFERENCES

Atkinson, G. D., and C. R. Holliday, 1975: Tropical cyclone minimum sea level pressure–maximum sustained wind relationship for western North Pacific. FLEWEACEN Tech. Note JTWC 75-1, U.S. Fleet Weather Central, Guam, 20 pp. [Available from National Meteorological Library, GPO Box 1289, Melbourne, VIC 3001, Australia.]

——, and ——, 1977: Tropical cyclone minimum sea level pressure/maximum sustained wind relationship for the western North Pacific. *Mon. Wea. Rev.,* **105,** 421–427.

Cocks, S. B., and W. M. Gray, 2002: Variability of the outer wind profiles of western North Pacific typhoons: Classifications and techniques for analysis and forecasting. *Mon. Wea. Rev.,* **130,** 1989–2005.

Dvorak, V. F., 1975: Tropical cyclone intensity analysis and forecasting from satellite imagery. *Mon. Wea. Rev.,* **103,** 420–430.

——, 1984: Tropical cyclone intensity analysis using satellite data. NOAA Tech. Rep. NESDIS 11, 45 pp.

Emanuel, K., 2005: Increasing destructiveness of tropical cyclones over the past 30 years. *Nature,* **436,** 686–688.

Franklin, J. L., M. L. Black, and K. Valde, 2003: GPS dropwindsonde wind profiles in hurricanes and their operational implications. *Wea. Forecasting,* **18,** 32–44.

Gross, J. M., M. DeMaria, J. A. Knaff, and C. R. Sampson, 2004: A new method for determining tropical cyclone wind forecast probabilities, Preprints, *26th Conf. on Hurricanes and Tropical Meteorology,* Miami, FL, Amer. Meteor. Soc., 425–426.

Guard, C. P., and M. A. Lander, 1996: A wind–pressure relationship for midget TCs in the western North Pacific. 1996 Annual Tropical Cyclone Rep., Naval Pacific Meteorology and Oceanography Center/Joint Typhoon Warning Center, 311 pp. [Available online at http://www.npmoc.navy.mil/jtwc/atcr/atcr_archive.html.]

Harper, B. A., 2002: Tropical cyclone parameter estimation and the Australian region: Wind–pressure relationships and related issues for engineering planning and design—A discussion paper. Systems Engineering Australia Rep. J0106-PR003E, 83 pp. [Available from Systems Engineering Australia Pty Ltd., 7 Mercury Ct., Bridgeman Downs, QLD 4035, Australia.]

Hess, S. L., 1959: *Introduction to Theoretical Meteorology.* Holt, Rinehart and Winston, 362 pp.

Jarvinen, B. R., C. J. Neumann, and M. A. S. Davis, 1984: A tropical cyclone data tape for the North Atlantic Basin, 1886-1983: Contents, limitations, and uses. NOAA Tech. Memo., NWS NHC-22, 21 pp. [Available from NTIS, 5285 Port Royal Rd., Springfield, VA 22161.]

JTWC, cited 2006: Tropical cyclone best track data site. [Available online at http://www.npmoc.navy.mil/jtwc/best_tracks/btwplink.html.]

Kalnay, E., and Coauthors, 1996: The NCEP/NCAR 40-Year Reanalysis Project. *Bull. Amer. Meteor. Soc.,* **77,** 437–471.

Kepert, J., 2001: The dynamics of boundary layer jets within the tropical cyclone core. Part I: Linear theory. *J. Atmos. Sci.,* **58,** 2469–2484.

——, and Y. Wang, 2001: The dynamics of boundary layer jets within the tropical cyclone core. Part II: Nonlinear enhancement. *J. Atmos. Sci.,* **58,** 2485–2501.

Knaff, J. A., M. DeMaria, and J. P. Kossin, 2003: Annular hurricanes. *Wea. Forecasting,* **18,** 204–223.

Koba, H., T. Hagiwara, S. Asano, and S. Akashi, 1990: Relationships between CI number from Dvorak's technique and minimum sea level pressure or maximum wind speed of tropical cyclone (in Japanese). *J. Meteor. Res.,* **42,** 59–67.

Kossin, J. P., 2002: Daily hurricane variability inferred from GOES infrared imagery. *Mon. Wea. Rev.,* **130,** 2260–2270.

Landsea, C. W., and Coauthors, 2004: The Atlantic hurricane database re-analysis project: Documentation for 1951–1910. Alterations and additions to the HURDAT. *Hurricanes and Typhoons Past, Present and Future,* R. J. Murname and K.-B. Liu, Eds., Columbia University Press, 177–221.

Love, G., and K. Murphy, 1985: The operational analysis of tropical cyclone wind fields in the Australian northern region. Northern Territory Region Research Papers 1984–85, Bureau of Meteorology, 44–51. [Available from National Meteorological Library, GPO Box 1289, Melbourne, VIC 3001, Australia.]

Lubeck, O. M., and J. D. Shewchuk, 1980: Tropical cyclone minimum sea level pressure maximum sustained wind relationship. NOCC/JTWC 80-1, USNOCC, JTWC, Pearl Harbor, HI, 96860. [Available from National Meteorological Library, GPO Box 1289, Melbourne, VIC 3001, Australia.]

Martin, J. D., and W. M. Gray, 1993: Tropical cyclone observation and forecasting with and without aircraft reconnaissance. *Wea. Forecasting,* **8,** 519–532.

Merrill, R. T., 1984: A comparison of large and small tropical cyclones. *Mon. Wea. Rev.,* **112,** 1408–1418.

Mueller, K. J., M. DeMaria, J. A. Knaff, J. P. Kossin, and T. H. Vonder Haar, 2006: Objective estimation of tropical cyclone wind structure from infrared satellite data. *Wea. Forecasting,* **21,** 990–1005.

Sampson, C. R., and A. J. Schrader, 2000: The Automated Tropical Cyclone Forecasting System (version 3.2). *Bull. Amer. Meteor. Soc.,* **81,** 1231–1240.

Schwerdt, R. W., F. P. Ho, and R. R. Watkins, 1979: Meteorological criteria for standard project hurricane and probable maximum hurricane wind fields—Gulf and East Coasts of the United States. NOAA Tech. Rep. NWS 23, 317 pp. [Available from National Hurricane/Tropical Prediction Center Library, 11691 S.W. 117th St., Miami, FL 33165-2149.]

Shewchuk, J. D., and R. C. Weir, 1980: An evaluation of the Dvorak technique for estimating tropical cyclone intensities from satellite imagery. NOCC/JTWC 80-2, USNOCC, JTWC, Pearl Harbor, HI, 25 pp. [Available from National Meteorological Library, GPO Box 1289, Melbourne, VIC 3001, Australia.]

Weatherford, C. L., and W. M. Gray, 1988: Typhoon structure as revealed by aircraft reconnaissance. Part II: Structural variability. *Mon. Wea. Rev.,* **116,** 1044–1056.

Webster, P. J., G. J. Holland, J. A. Curry, and H.-R. Chang, 2005: Changes in tropical cyclone number, duration, and intensity in a warming environment. *Science,* **309,** 1844–1846.

Willoughby, H. E., 1990: Gradient balance in tropical cyclones. *J. Atmos. Sci.,* **47,** 265–274.

——, and M. E. Rahn, 2004: Parametric representation of the primary hurricane vortex. Part I: Observations and evaluation of the Holland (1980) model. *Mon. Wea. Rev.,* **132,** 3033–3048.